Erratum

A constitutive model for air–NAPL–water flow in the vadose zone accounting for immobile, non-occluded (residual) NAPL in strongly water-wet porous media[☆]

R.J. Lenhard[a,*], M. Oostrom[b], J.H. Dane[c]

[a] Subsurface Science Initiative, Idaho National Engineering and Environmental Laboratory (INEEL),
PO Box 1625, MS 2025, Idaho Falls, ID 83415-2025, USA
[b] Environmental Technology Division, PNNL, PO Box 999, K9-33, Richland, WA, USA
[c] Agronomy and Soils Department, Auburn University, Auburn, AL, USA

Abstract

A hysteretic constitutive model describing relations among relative permeabilities, saturations, and pressures in fluid systems consisting of air, nonaqueous-phase liquid (NAPL), and water is modified to account for NAPL that is postulated to be immobile in small pores and pore wedges and as films or lenses on water surfaces. A direct outcome of the model is prediction of the NAPL saturation that remains in the vadose zone after long drainage periods (residual NAPL). Using the modified model, water and NAPL (free, entrapped by water, and residual) saturations can be predicted from the capillary pressures and the water and total-liquid saturation-path histories. Relations between relative permeabilities and saturations are modified to account for the residual NAPL by adjusting the limits of integration in the integral expression used for predicting the NAPL relative permeability. When all of the NAPL is either residual or entrapped (i.e., no free NAPL), then the NAPL relative permeability will be zero. We model residual NAPL using concepts similar to those used to model residual water. As an initial test of the constitutive model, we compare predictions to published measurements of residual NAPL. Furthermore, we present results using the modified constitutive theory for a scenario involving NAPL imbibition and drainage.
© 2003 Elsevier B.V. All rights reserved.

Keywords: Residual NAPL; Constitutive theory; Relative permeability relations; Three-phase flow; NAPL flow

---

* Corresponding author.
E-mail address: lenhrj@inel.gov (R.J. Lenhard).

1. Background

Modeling the subsurface behavior of contaminants can be a cost-effective tool to aid in cleaning up and managing contaminated sites. Before models can be the tools of choice, they must be able to accurately predict contaminant behavior and assess the level of uncertainty associated with the predictions. One shortcoming of multifluid flow and transport codes is their inability to accurately predict the retention of nonaqueous-phase liquid (NAPL) in the vadose zone after long drainage periods. Conceptually, this NAPL is present in small pores, pore wedges, bypassed pores, and as films or lenses on water or solid surfaces. In Fig. 1, we show a cartoon of the various forms of NAPL that might not drain from pores in the vadose zone after long drainage periods in a strongly water-wet porous medium.

We contend that the inability to accurately predict NAPL distribution in the vadose zone is a consequence of deficiencies in the multifluid air–NAPL–water constitutive theory (relations among relative permeabilities, saturations, and pressures) employed in numerical simulators. It is common to assume that all NAPL is mobile unless it is occluded (surrounded) by water and exists as ganglia (entrapped NAPL). However, experimental investigations (Hofstee et al., 1998; Oostrom and Lenhard, 2003; Oostrom et al., 2003) have shown that nonwater-occluded NAPL is retained in the vadose zone after NAPL drainage has ceased. We postulate that this nonwater-occluded NAPL remains in
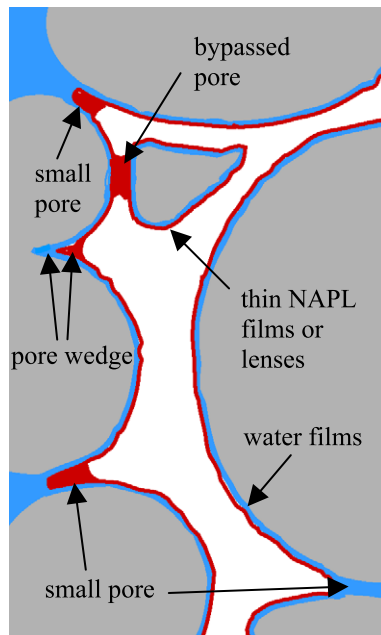

Fig. 1. A cartoon depicting conceptual forms of NAPL (i.e., NAPL-filled small pores, NAPL-filled pore wedges, NAPL films or lenses on water films, and NAPL-filled bypassed pores) that may not drain from the vadose zone after long periods of drainage. The immobile NAPL is red, water is blue, air is white, and solid particles are grey.

the vadose zone because it exists in forms that are immobile or negligibly mobile. Such forms include films or lenses on water surfaces, NAPL in small or 'dead-end' pore channels and pore wedges, and NAPL in bypassed pores (Fig. 1). By accounting for these immobile forms of nonwater-occluded NAPL in relative permeability–saturation–pressure (k–S–P) relations, it should be possible to predict the NAPL saturation that does not drain from the vadose zone after long drainage periods. Vadose-zone hydrologists have used the term 'residual NAPL' to describe nonwater-occluded NAPL that does not drain from the vadose zone after long drainage periods (Cary et al., 1989; Poulsen and Kueper, 1992; Cohen and Mercer, 1993; Jarsjo et al., 1994; Hofstee et al., 1997; Wipfler and van der Zee, 2001; van Geel and Roy, 2002—among others).

Residual saturation is a term used by modelers in the hydrologic and petroleum sciences to describe different phenomena or processes. Use of this term can be confusing unless supporting information is given, such as the wettability of the porous medium. When applied to water in strongly water-wet porous media, the residual-water saturation is the water saturation at which the water relative permeability decreases to zero. Theoretically, it refers to the water contained in the smallest pore spaces (pore wedges, pores) and as films on solid surfaces (Fig. 1). It is the minimum water content that can be obtained by water (liquid) drainage when there are no restrictions to drainage (e.g., capillary breaks, impermeable layers). In the petroleum industry, the residual-water saturation is also referred to as the irreducible-water saturation. As far as we can determine, the concept of a residual- or irreducible-water saturation was first discussed in the late 1940s and early 1950s by a number of investigators (e.g., Rose, 1949; Rose and Bruce, 1949; Rapoport and Leas, 1951; Wyllie and Sprangler, 1952; Burdine, 1953).

When applied to NAPL in strongly water-wet porous media, the term 'residual NAPL' has been used to describe the NAPL saturation that becomes occluded by water as water displaces NAPL into larger pore spaces during water imbibition (Fig. 2, entrapped NAPL). Additionally, 'residual NAPL' has been applied to describe the NAPL saturation in the vadose zone that does not drain from the pore spaces when no drainage restrictions exist. In strongly water-wet porous media, the NAPL is a nonwetting fluid. Typically, the vadose zone is assumed to be strongly water wet. 'Residual NAPL' has also been applied to mixed- and oil-wet porous media in the petroleum industry (Salathiel, 1973; Willhite, 1986; Anderson, 1987; Morrow, 1990; Kovscek et al., 1993). In those systems, the residual-NAPL saturation is similar in concept to the residual-water saturation in strongly water-wet porous media (NAPL is contained in the smallest pore spaces available) because it is the wetting fluid in the oil-wet pore spaces. 'Residual NAPL' is a term that is used by various disciplines (e.g., petroleum versus vadose-zone hydrologists) to describe different processes. It has been used to describe either a nonwetting or a wetting fluid and is conceptualized as being continuous, discontinuous, or both throughout the pore spaces. In all cases, however, the 'residual' NAPL is considered to be immobile.

In the following discussions, we will employ the definition of 'residual NAPL' used by vadose-zone hydrologists for strongly water-wet porous media. We will call NAPL that is occluded by water as *entrapped NAPL* (Fig. 2) and NAPL that is not entrapped by water, but does not drain from the pore spaces, as *residual NAPL* (Fig. 1). *Entrapped NAPL* could also be called 'occluded residual NAPL' and *residual NAPL* could be called 'non-occluded residual NAPL'. Both forms of NAPL (entrapped and residual) are assumed to be
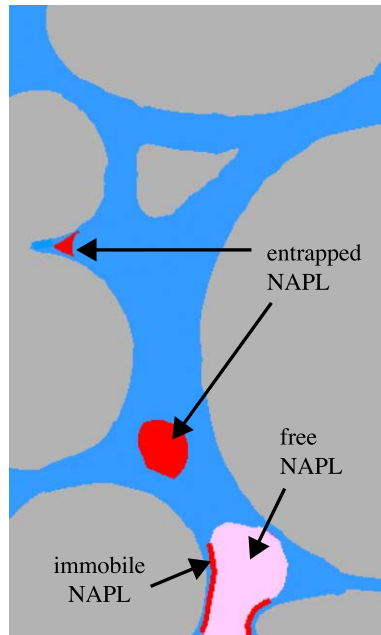
Fig. 2. A cartoon depicting water imbibition in the pore spaces. Some NAPL becomes occluded by water and immobile (red), while the free NAPL (pink) is displaced into larger pore spaces. The water-occluded NAPL is called entrapped NAPL. Water is blue and solid particles are grey.

immobile. Residual NAPL can be discontinuous and/or continuous throughout the pore spaces, but entrapped NAPL is always discontinuous.

Residual and entrapped NAPL are important because they are long-term sources of groundwater contamination. Two research groups (Wipfler and van der Zee, 2001; van Geel and Roy, 2002) have recently proposed amendments to existing multifluid consti-tutive theory in order to predict the residual-NAPL saturation. In the model proposed by Wipfler and van der Zee (2001), a critical NAPL pressure is defined from knowledge of a critical total-liquid saturation, which depends on the fluids and porous medium. The critical NAPL pressure defines the transition from free (mobile) NAPL to residual (immobile) NAPL. Wipfler and van der Zee (2001) do not address relative permeability relations. Van Geel and Roy (2002) conducted a series of saturation–pressure $(S–P)$ measurements to investigate residual NAPL, and they utilized their data to develop a model to predict the residual-NAPL saturation. Their model is based on knowledge of the maximum residual-NAPL saturation, the apparent total-liquid saturation, and the apparent total-liquid saturation at the saturation-path reversal from the primary wetting $S–P$ curve to a drainage $S–P$ scanning curve. Their predictive equation does not explicitly include the water saturation. By defining the total-NAPL saturation to be the sum of free-, entrapped-, and residual-NAPL saturations, they indirectly address relative permeability relations. When all of the NAPL becomes residual and entrapped, the NAPL relative permeability goes to zero because the free-NAPL saturation is zero.

In this paper, we present a model to account for the effects of immobile, nonwater-occluded NAPL (residual NAPL) on NAPL behavior in the subsurface. Our model differs from that of Wipfler and van der Zee (2001) because free and residual NAPL can coexist in the pore spaces. In their model, free and residual NAPL cannot coexist. Our model differs from that of van Geel and Roy (2002) because we hypothesize that the water saturation is an important variable and should be explicitly included in any equation for predicting residual NAPL. Our model is developed to be consistent with the hysteretic constitutive theory for k–S–P relations developed by Parker and Lenhard (1987) and Lenhard and Parker (1987). We test the modified S–P relations by calculating residual-NAPL saturations for the experimental conditions reported in van Geel and Roy (2002) and compare those predictions to van Geel and Roy's measurements. Additionally, we demonstrate the use of the modified model for a scenario involving NAPL imbibition and subsequent drainage to its residual value.

2. Conceptual model

Our objective is to improve existing multifluid constitutive theory (i.e., k–S–P relations) so that the effects of entrapped and residual NAPL on subsurface contamination
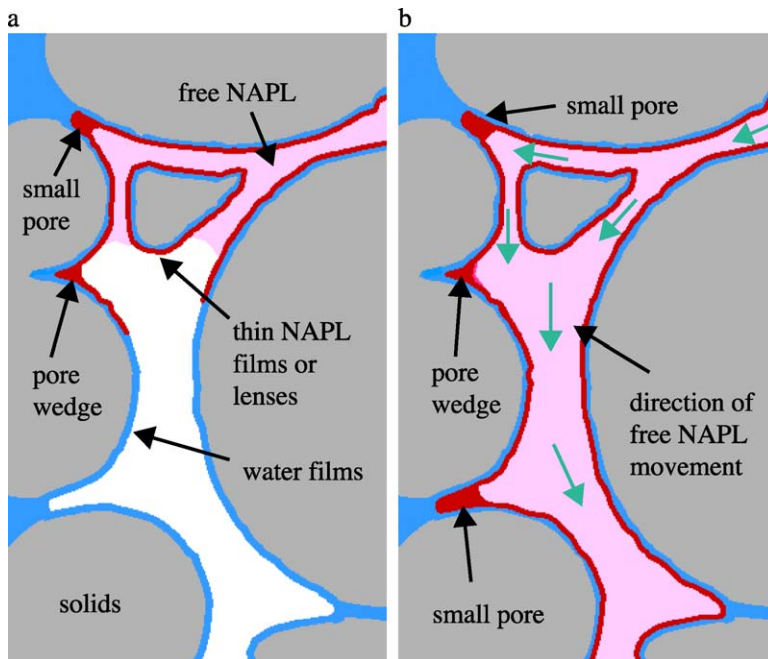

Fig. 3. Cartoons depicting NAPL imbibition in the pore spaces. In (a), small pores and pore wedges are filled with NAPL before the larger pore bodies are filled. After these smaller spaces are filled, the NAPL is assumed to be immobile (red). In (b), the pore system is NAPL-filled with the mobile (free) NAPL shown as pink. Water is blue and solid particles are grey.

and cleanup can be predicted. However, we first want to give a conceptual understanding of 'residual' NAPL, as we will use it in our model.

We hypothesize that NAPL in small pores and small pore wedges can be considered to be immobile because (1) the pore dimensions are small and any advection of NAPL through those spaces would be negligible or (2) the pore spaces are 'dead-end' channels that are unable to conduct NAPL. We also hypothesize that NAPL adjacent to water films that are adsorbed to solid particles do not effectively contribute to NAPL advection and can be considered to be immobile (Fig. 3), especially if the water films are thin. We reason that there is no significant 'slippage' along the NAPL–water interface after the NAPL wets water films. Therefore, the NAPL at the interface should move at the same velocity as the water at the interface, which would likely be negligible relative to the velocity of NAPL at the centers of the pores.

Once the small pores and pore wedges are filled with NAPL and the NAPL films are formed (Fig. 3a), the NAPL in those spaces becomes practically immobile. Therefore, the 'residual' NAPL forms during NAPL imbibition, not during drainage. We do not feel that NAPL in small pores and pore wedges, and as films on water surfaces, are mobile during NAPL imbibition, but immobile during drainage. After forming, the 'residual' NAPL does not contribute to NAPL advection whether the NAPL is imbibing or draining. In a pore system filled with NAPL, some NAPL can potentially move and some NAPL is assumed to be immobile. We call the NAPL that can potentially move 'free' NAPL and we call the nonwater-occluded NAPL, assumed to be immobile, 'residual' NAPL (Fig. 3b).

3. Model development

We will modify the hysteretic, multifluid $k–S–P$ model of Parker and Lenhard (1987) and Lenhard and Parker (1987), which is valid for air–NAPL–water systems in strongly water-wet porous media where water is the wetting fluid and air and NAPL are nonwetting fluids with NAPL wetting water surfaces relative to air. The intent is to minimize changes to the existing model so that coding the improvements will not be a major undertaking, but the use of the model in flow and transport simulators will yield results that more accurately reflect NAPL behavior in the field.

It is appropriate to first give definitions of saturation terms that will be used in the model because both apparent and effective saturations are used and readers may not be familiar with the existing model. An apparent saturation is a scaled fluid saturation that is corrected (adjusted) for entrapped fluids. An effective saturation is a scaled saturation that is not corrected for entrapped fluids. Typically, an effective saturation refers to a single fluid form (e.g., water, entrapped air), whereas an apparent saturation includes multiple fluid forms because it accounts for entrapped fluids. Apparent saturations are used to obtain a more accurate description of the distribution of fluids in the pore spaces. The apparent water saturation is predicted from the NAPL–water capillary pressure and the water saturation-path history. The apparent total-liquid saturation is predicted from the air–NAPL capillary pressure and the total-liquid saturation-path history. The entrapped and non-entrapped saturations are determined from the apparent saturations and saturation-

path histories. Readers are referred to Parker and Lenhard (1987), Lenhard and Parker (1987), and Lenhard (1992) for further discussion of effective and apparent saturations.

3.1. Saturation definitions

The apparent water saturation is defined as

$$\bar{\bar{S}}_{\mathrm{w}} = \frac{S_{\mathrm{w}} + S_{\mathrm{oe}} + S_{\mathrm{aew}} - S_{\mathrm{wr}}}{1 - S_{\mathrm{wr}}} \tag{1}$$

where S_{w} is the water saturation, S_{oe} is the entrapped-NAPL saturation (occluded by water), S_{aew} is the entrapped-air saturation in water (occluded by water), and S_{wr} is the residual-water saturation, which is assumed to be immobile and the value of which is independent of the water saturation-path history. The entrapped-NAPL saturation in water (S_{oe}) includes the entrapped air in the entrapped NAPL that is occluded by water.

The apparent total-liquid saturation is defined as

$$\bar{\bar{S}}_{\mathrm{t}} = \frac{S_{\mathrm{w}} + S_{\mathrm{o}} + S_{\mathrm{ae}} - S_{\mathrm{wr}}}{1 - S_{\mathrm{wr}}} \tag{2}$$

where S_{o} is the total-NAPL saturation and S_{ae} is the total entrapped-air saturation. The total entrapped-air saturation (S_{ae}) is the sum of entrapped-air saturations occluded by water and occluded by the NAPL, i.e.,

$$S_{\mathrm{ae}} = S_{\mathrm{aew}} + S_{\mathrm{aeo}} \tag{3}$$

where S_{aeo} is the entrapped-air saturation occluded by the NAPL, which is not also occluded by water (not the entrapped air in the entrapped NAPL). The values of S_{oe}, S_{aew}, and S_{ae} in Eqs. (1) and (2) are functions of the water and total-liquid saturation-path histories (see Lenhard, 1992 for details). Equations (1)–(3) are given for the convenience of the reader; the definitions of the apparent water and total-liquid saturations are unchanged from the existing model.

The modifications to the constitutive theory are presented in two sections. The first section (3.2) describes changes to the $S-P$ submodel and the second section (3.4) describes changes to the $k-S$ submodel. We refer to the $S-P$ relations described in Parker and Lenhard (1987) and Lenhard (1992) and the $k-S$ relations described in Lenhard and Parker (1987) as the 'existing' models.

3.2. S–P submodel

The major modification to the existing $S-P$ model is to divide the nonwater-occluded NAPL into free (mobile) and residual (immobile) components and to predict the residual component using the total-liquid and water saturation-path histories. In the existing model, the total-NAPL saturation consists of two components: free- and entrapped-NAPL saturations. The free-NAPL saturation is mobile and the entrapped-NAPL saturation is immobile. In our modification, we define the total-NAPL saturation to consist of three components: free-, entrapped-, and residual-NAPL saturations. The free-NAPL saturation is the portion of the NAPL that is continuous and mobile with regard to NAPL advection.

The entrapped-NAPL saturation is the portion of the NAPL consisting of discontinuous, immobile ganglia occluded by water. The residual-NAPL saturation is the portion of the NAPL that is not occluded by water, but is immobile. We redefine the total-NAPL saturation as

$$S_o = S_{of} + S_{oe} + S_{or} \tag{4}$$

where S_{of} is the free-NAPL saturation, S_{oe} is the entrapped-NAPL saturation, and S_{or} is the residual-NAPL saturation. The symbol S_{or} in the existing model is used to denote the maximum amount of water-occluded NAPL with coexisting entrapped air for a given water saturation-path history. Using symbols consistent with this manuscript, the symbol S_{or} in the existing model should be replaced with S_{oe}^{max}. Van Geel and Roy (2002) used the same definition for total-NAPL saturation (S_o) that we use in Eq. (4). To determine the total-NAPL saturation (S_o), each component on the right-hand side of Eq. (4) needs to be calculated based on the total-liquid and water saturation-path histories and the NAPL–water and air–NAPL capillary pressures. The total-NAPL saturation (S_o) does not approach zero when the free-NAPL saturation (S_{of}) approaches zero.

3.3. Residual saturation

We theorize that the residual-NAPL saturation depends largely on two factors. The first factor is related to the volume of pore space occupied by NAPL, while the second factor is related to the size of the pores containing the NAPL. We propose that these factors affect the value of the residual-NAPL saturation in a nonlinear manner. Accordingly, we propose that the residual-NAPL saturation can be predicted using a power function of the form

$$\bar{S}_{or} = AB^\lambda C^\eta = \frac{S_{or}}{1 - S_{wr}} \tag{5}$$

where $\bar{S}_{or}$ is the effective residual-NAPL saturation, A is a calibration term that reflects the maximum residual-NAPL saturation possible for a porous medium, B is a factor related to the volume of pore space occupied by NAPL, C is a factor related to the size of the pores containing the NAPL, and λ and η are power law exponents.

The calibration term (A) in Eq. (5) is related to the maximum residual-NAPL saturation (S_{or}^{max}) that can be obtained in a porous medium. It is porous medium and fluid-specific. We will use the B and C terms in Eq. (5) to scale the maximum residual-NAPL saturation (the A term) to predict the effective residual-NAPL saturation for given conditions. The maximum residual-NAPL saturation (S_{or}^{max}) can be measured by draining water to its residual-water saturation in a two-phase NAPL–water fluid system that is initially water-saturated, followed by draining NAPL to its residual-NAPL saturation. For spreading NAPLs (NAPLs for which the sum of the NAPL–water and air–NAPL interfacial tensions is equal to or less than the air–water interfacial tension), the NAPL will form a film (will spread) on the water surfaces when the maximum residual-NAPL saturation (S_{or}^{max}) is measured. For nonspreading NAPLs (NAPLs for which the sum of the NAPL–water and air–NAPL interfacial tensions is greater than the air–water interfacial tension), the NAPL will form lenses on the water surfaces when the maximum residual-NAPL saturation (S_{or}^{max}) is measured. We reason that the different behavior of spreading and nonspreading NAPLs in porous media can be addressed via the calibration term (A) in Eq. (5). Measurement systems similar to those described by Lenhard and Parker (1988), Busby

et al. (1995), and van Geel and Roy (2002) can be used to determine the maximum residual-NAPL saturation (S_{or}^{max}). After S_{or}^{max} is measured, it must be scaled to yield an effective saturation using

$$A = \bar{S}_{or}^{max} = \frac{S_{or}^{max}}{1 - S_{wr}} \tag{6}$$

The term B in Eq. (5) is a measure of the volume fraction of pore space occupied by NAPL. An expression for B must ensure that it is 0 when the residual-NAPL saturation (S_{or}) is 0 and that it is 1 when S_{or} is at its maximum for a given water saturation-path history. Accordingly, we propose the relationship

$$B = \frac{\bar{\bar{S}}_t^{max} - \bar{\bar{S}}_w}{1 - \bar{\bar{S}}_w} \tag{7}$$

where $\bar{\bar{S}}_t^{max}$ is the historic maximum apparent total-liquid saturation in an air–NAPL–water fluid system. Using Eq. (7), $B=0$ when the apparent water saturation ($\bar{\bar{S}}_w$) is equal to the historic maximum apparent total-liquid saturation ($\bar{\bar{S}}_t^{max}$), which occurs when either NAPL imbibes into a two-phase air–water system or when all of the NAPL becomes entrapped in water. In both cases, conditions are such that the residual-NAPL saturation (S_{or}) is 0. The apparent water saturation ($\bar{\bar{S}}_w$) can never be greater than the historic maximum apparent total-liquid saturation ($\bar{\bar{S}}_t^{max}$) because it would mean that the apparent water saturation is greater than the apparent total-liquid saturation ($\bar{\bar{S}}_t$), which is physically impossible. The largest residual-NAPL saturation for a given water saturation-path history will occur when the historic maximum apparent total-liquid saturation ($\bar{\bar{S}}_t^{max}$) is 1. For the conditions that pertain to measuring the maximum residual-NAPL saturation (S_{or}^{max}), B is also 1 because $\bar{\bar{S}}_t^{max}=1$ and $S_w=S_{wr}$. When conducting numerical simulations, the historic maximum apparent total-liquid saturation ($\bar{\bar{S}}_t^{max}$) needs to be updated after every time step for each node.

The term C in Eq. (5) is a measure of the size (radii) of the pores containing the NAPL. We use this measure to estimate the volume of NAPL that is immobile in thin films or lenses on water surfaces. Again, this term must be 0 when the residual-NAPL saturation (S_{or}) is 0 and be 1 when S_{or} is a maximum ($S_{or}=S_{or}^{max}$). For the former constraint, immobile NAPL in thin films or lenses on water surfaces will only be zero when the apparent water saturation ($\bar{\bar{S}}_w$) is 1 or when a two-phase air–water system exists. For the latter constraint, the maximum value of immobile NAPL in thin films or lenses on water surfaces should theoretically occur when the apparent water saturation ($\bar{\bar{S}}_w$) is 0—the water saturation (S_w) is equal to the residual-water saturation (S_{wr}). An expression that meets these constraints is

$$C = (1 - \bar{\bar{S}}_w) \tag{8}$$

Substituting expressions for A, B, and C (Eqs. (6)–(8)) into Eq. (5), the following equation for predicting the effective residual-NAPL saturation as a function of saturation-path history is obtained:

$$\bar{S}_{or} = \bar{S}_{or}^{max} \left(\frac{\bar{\bar{S}}_t^{max} - \bar{\bar{S}}_w}{1 - \bar{\bar{S}}_w} \right)^{\lambda} (1 - \bar{\bar{S}}_w)^{\eta} \tag{9}$$

To determine the power law exponent λ in Eq. (9), we hypothesize that immobile NAPL in pore wedges and in small pores will increase as the volume of pore space that contains NAPL increases. As the NAPL invades larger-sized pores, small pores can become accessible to the NAPL that otherwise would not be accessible. However, the rate of increase in residual NAPL will decrease as the volume of pore space that contains NAPL becomes larger (the volume of pore space in pore wedges and in small pores relative to the total pore volume will decrease as NAPL invades larger pores). Consequently, we propose using $\lambda = 0.5$ as a first approximation. To determine the power law exponent η in Eq. (9), we hypothesize that the volume of immobile NAPL in thin films or lenses on water surfaces will be greater when NAPL is in smaller radii pore spaces relative to larger radii pore spaces (more surface area in a given volume). As smaller radii pores become accessible to the NAPL because of water drainage, then the volume of immobile NAPL in thin films or lenses on water surfaces will increase at an increasing rate. Accordingly, we propose using $\eta = 2$ based on the hypothesis that the increase in the volume of NAPL present in thin films or as lenses on water surfaces as the apparent water saturation ($\bar{\bar{S}}_w$) becomes smaller follows a pattern similar to the variation of tortuosity as the water saturation decreases, as proposed by Burdine (1953).

Substituting the proposed values for λ and η in Eq. (9), the following predictive equation for the effective residual-NAPL saturation is

$$\bar{S}_{or} = \bar{S}_{or}^{max}(\bar{\bar{S}}_t^{max} - \bar{\bar{S}}_w)^{0.5}(1 - \bar{\bar{S}}_w)^{1.5} \tag{10}$$

The only other modification needed for the existing model addresses air entrapment. In the existing model, entrapped air is a function of the total-NAPL saturation. In our modification, we assume that all entrapped air in the NAPL (i.e., S_{aeo}) is entrapped only by the free NAPL and not by any residual NAPL. Therefore, entrapped air in NAPL should be a function of the free-NAPL saturation and not the total-NAPL saturation.

3.4. k–S submodel

Using the modifications in the S–P model, k–S relations can be predicted using an approach similar to that used in the existing model. Predictions of the water and air relative permeabilities are identical to those in the existing model. The major modification is in the determination of the NAPL relative permeability (k_{ro}). The key assumption is that all of the residual NAPL is contained in pore spaces indexed between the apparent water saturation ($\bar{\bar{S}}_w$) and the sum of the apparent water saturation and the effective residual-NAPL saturation ($\bar{\bar{S}}_w + \bar{S}_{or}$). This assumption is necessary to obtain an expedient method to predict the NAPL relative permeability. If we knew how the residual NAPL is distributed throughout the pore spaces indexed between the historic maximum apparent total-liquid saturation ($\bar{\bar{S}}_t^{max}$) and the apparent water saturation ($\bar{\bar{S}}_w$), then we could develop a protocol for estimating the NAPL relative permeability (k_{ro}) that reflects the distribution of discontinuous and continuous residual NAPL in porous media. In the absence of a well-defined theory describing the distribution of residual NAPL, we have used the above assumption as a first approximation.

Applying the above assumption to Mualem's (1976) integral expression for relative permeability to account for effects of residual NAPL and entrapped air on the NAPL relative permeability (k_{ro}), the integral expression becomes

$$k_{ro} = \bar{S}_{of}^{0.5} \left\{ \frac{\int_{\bar{\bar{S}}_w + \bar{S}_{or}}^{\bar{\bar{S}}_t} \frac{d\bar{S}_e}{h(\bar{S}_e)} - \int_0^{\bar{S}_{aeo}} \frac{d\bar{S}_{aeo}}{h(\bar{S}_e)}}{\int_0^1 \frac{d\bar{S}_e}{h(\bar{S}_e)}} \right\}^2 \tag{11}$$

where $\bar{S}_{aeo}$ is the effective entrapped-air saturation in the free NAPL, $\bar{S}_e$ is the effective porosity in which the flow of the fluid under consideration can potentially occur, and $h(\bar{S}_e)$ is a surrogate for the pore-size distribution of the porous medium. The limits of integration are chosen so that the integration of the relative permeability integral is performed only over the pore space containing mobile NAPL. Both the effective free-NAPL saturation term (tortuosity term) and the integrals in the numerator of Eq. (11) will approach zero as the free-NAPL saturation (S_{of}) approaches zero. In the model proposed by van Geel and Roy (2002), only the tortuosity term approaches zero as S_{of} approaches zero.

Following Lenhard and Parker (1987), the integral on the right-hand side in the numerator of Eq. (11), which corrects for obstruction of NAPL flow by the entrapped air in the free NAPL, can be expressed in terms of $\bar{S}_e$ for different saturation-path histories. For saturation-path histories for which all of the free NAPL is in pores that were previously occupied by air in the air–NAPL–water system ($\bar{\bar{S}}_w + \bar{S}_{or} \geq \bar{\bar{S}}_t^{min}$), the transformation yields

$$\int_0^{\bar{S}_{aeo}} \frac{d\bar{S}_{aeo}}{h(\bar{S}_e)} = \frac{\bar{S}_{aeo}^{max}}{1 - \bar{\bar{S}}_t^{min}} \int_{\bar{\bar{S}}_w + \bar{S}_{or}}^{\bar{\bar{S}}_t} \frac{d\bar{S}_e}{h(\bar{S}_e)} \tag{12}$$

where $\bar{S}_{aeo}^{max}$ is the effective maximum entrapped-air saturation that resulted from advancing air–NAPL interfaces and $\bar{\bar{S}}_t^{min}$ is the historic minimum apparent total-liquid saturation. The effective maximum entrapped-air saturation ($\bar{S}_{aeo}^{max}$) is a function of the historic minimum apparent total-liquid saturation ($\bar{\bar{S}}_t^{min}$).

For saturation-path histories for which only some of the free NAPL is in pores that were previously occupied by air in the air–NAPL–water system and the remainder of the free NAPL is in smaller pores that were previously occupied by air in the air–water system ($\bar{\bar{S}}_w + \bar{S}_{or} < \bar{\bar{S}}_t^{min}$ and $\bar{\bar{S}}_t^{min} \geq {}^{\Delta}\bar{S}_w^{aw}$), the transformation yields

$$\int_0^{\bar{S}_{ato}} \frac{d\bar{S}_{aeo}}{h(\bar{S}_e)} = \frac{\bar{S}_{aew}^{max}}{1 - {}^{\Delta}\bar{S}_w^{aw}} \int_{\Psi}^{\bar{\bar{S}}_t^{min}} \frac{d\bar{S}_e}{h(\bar{S}_e)} + \frac{\bar{S}_{aeo}^{max}}{1 - \bar{\bar{S}}_t^{min}} \int_{\bar{\bar{S}}_t^{min}}^{\bar{\bar{S}}_t} \frac{d\bar{S}_e}{h(\bar{S}_e)} \tag{13}$$

where $\bar{S}_{aew}^{max}$ is the effective maximum entrapped-air saturation that resulted from advancing air–water interfaces, ${}^{\Delta}\bar{S}_w^{aw}$ is the effective water saturation at the saturation-path reversal from the main $S–P$ path to a scanning water imbibition path in a two-phase air–water fluid system, and Ψ is the maximum of either $\bar{\bar{S}}_w + \bar{S}_{or}$ or ${}^{\Delta}\bar{S}_w^{aw}$.

For saturation-path histories for which only some of the free NAPL is in pores that were previously occupied by air in the air−NAPL−water system and the remainder of the free NAPL is in smaller pores that were never occupied by air in either the air−water or air−NAPL−water systems ($\bar{\bar{S}}_w + \bar{S}_{or} < \bar{\bar{S}}_t^{min}$ and $\bar{\bar{S}}_t^{min} < {}^{\Delta}\bar{S}_w^{aw}$), the transformation yields

$$\int_0^{\bar{S}_{aeo}} \frac{d\bar{S}_{aeo}}{h(\bar{S}_e)} = \frac{\bar{S}_{aeo}^{max}}{1 - \bar{\bar{S}}_t^{min}} \int_\Omega^{\bar{\bar{S}}_t} \frac{d\bar{S}_e}{h(\bar{S}_e)} \tag{14}$$

where Ω is the maximum of either $\bar{\bar{S}}_w + \bar{S}_{or}$ or $\bar{\bar{S}}_t^{min}$.

Following van Genuchten (1980), closed-form expressions for the NAPL relative permeability (k_{ro}) of different saturation-path histories that account for residual NAPL are obtained by substituting Eqs. (12)–(14) into Eq. (11) and integrating.

For the condition $\bar{\bar{S}}_w + \bar{S}_{or} \geq \bar{\bar{S}}_t^{min}$, the solution is

$$k_{ro} = \bar{S}_{of}^{0.5} \left\{ \begin{array}{l} \left[1 - (\bar{\bar{S}}_w + \bar{S}_{or})^{1/m}\right]^m \left(1 - \dfrac{\bar{S}_{aeo}^{max}}{1 - \bar{\bar{S}}_t^{min}}\right) \\[2em] -(1 - \bar{\bar{S}}_t^{1/m})^m \left(1 - \dfrac{\bar{S}_{aeo}^{max}}{1 - \bar{\bar{S}}_t^{min}}\right) \end{array} \right\}^2 \tag{15}$$

where m is a parameter of the van Genuchten (1980) $S-P$ equation.

For the condition $\bar{\bar{S}}_w + \bar{S}_{or} < \bar{\bar{S}}_t^{min}$ and $\bar{\bar{S}}_t^{min} \geq {}^{\Delta}\bar{S}_w^{aw}$, the solution is

$$k_{ro} = \bar{S}_{of}^{0.5} \left\{ \begin{array}{l} \left[1 - (\bar{\bar{S}}_w + \bar{S}_{or})^{1/m}\right]^m - (1 - \bar{\bar{S}}_t^{1/m})^m \left(1 - \dfrac{\bar{S}_{aeo}^{max}}{1 - \bar{\bar{S}}_t^{min}}\right) \\[2em] -\left[1 - (\bar{\bar{S}}_t^{min})^{1/m}\right]^m \left[\dfrac{\bar{S}_{aeo}^{max}}{1 - \bar{\bar{S}}_t^{min}} - \dfrac{\bar{S}_{aew}^{max}}{1 - {}^{\Delta}\bar{S}_w^{aw}}\right] \\[2em] -(1 - \Psi^{1/m})^m \left(\dfrac{\bar{S}_{aew}^{max}}{1 - {}^{\Delta}\bar{S}_w^{aw}}\right) \end{array} \right\}^2 \tag{16}$$

For the condition $\bar{\bar{S}}_w + \bar{S}_{or} < \bar{\bar{S}}_t^{min}$ and $\bar{\bar{S}}_t^{min} < {}^{\Delta}\bar{S}_w^{aw}$, the solution is

$$k_{ro} = \bar{S}_{of}^{0.5} \left\{ \begin{array}{l} \left[1 - (\bar{\bar{S}}_w + \bar{S}_{or})^{1/m}\right]^m - (1 - \bar{\bar{S}}_t^{1/m})^m \left(1 - \dfrac{\bar{S}_{aeo}^{max}}{1 - \bar{\bar{S}}_t^{min}}\right) \\[2em] -(1 - \Omega^{1/m})^m \left(\dfrac{\bar{S}_{aeo}^{max}}{1 - \bar{\bar{S}}_t^{min}}\right) \end{array} \right\}^2 \tag{17}$$

A stepwise approach to evaluating the above conditional statements is needed when determining the NAPL relative permeability (k_{ro}) in order to minimize the number of conditional statements that must be evaluated. The conditional statement $\bar{\bar{S}}_w + \bar{S}_{or} \geq \bar{\bar{S}}_t^{min}$

needs to be evaluated first, followed by the second conditional statement ($\bar{\bar{S}}_w + \bar{S}_{or} < \bar{\bar{S}}_t^{min}$ and $\bar{\bar{S}}_t^{min} \geq {}^{\Delta}\bar{S}_w^{aw}$), and subsequently by the last statement ($\bar{\bar{S}}_w + \bar{S}_{or} < \bar{\bar{S}}_t^{min}$ and $\bar{\bar{S}}_t^{min} < {}^{\Delta}\bar{S}_w^{aw}$). For saturation-path histories other than $\bar{\bar{S}}_w + \bar{S}_{or} > \bar{\bar{S}}_t^{min}$, the apparent total-liquid saturation ($\bar{\bar{S}}_t$) will become equal to the historic minimum apparent total-liquid saturation ($\bar{\bar{S}}_t^{min}$) before $\bar{\bar{S}}_t$ becomes equal to $\bar{\bar{S}}_w + \bar{S}_{or}$ as $\bar{\bar{S}}_t$ approaches $\bar{\bar{S}}_w + \bar{S}_{or}$. When $\bar{\bar{S}}_t$, $\bar{\bar{S}}_t^{min}$, and $\bar{\bar{S}}_w + \bar{S}_{or}$ are equal to each other, which means that all of the NAPL becomes residual NAPL, then the first conditional statement will apply. The first conditional statement will always hold when the apparent total-liquid saturation ($\bar{\bar{S}}_t$) is equal to the sum of the apparent water saturation and the effective residual-NAPL saturation ($\bar{\bar{S}}_t = \bar{\bar{S}}_w + \bar{S}_{or}$). The predicted NAPL relative permeability (k_{ro}) will be zero for this condition [see Eq. (15) for the condition $\bar{\bar{S}}_t = \bar{\bar{S}}_w + \bar{S}_{or}$]. For the other solutions given by Eqs. (16) and (17), the NAPL relative permeability (k_{ro}) will never be zero because the apparent total-liquid saturation ($\bar{\bar{S}}_t$) can never be equal to the sum of the apparent water saturation and the effective residual-NAPL saturation ($\bar{\bar{S}}_t = \bar{\bar{S}}_w + \bar{S}_{or}$) for these saturation-path histories.

4. Discussion

Key elements of the proposed model are (1) some portion of the NAPL is predicted to remain in the pore spaces as residual NAPL unless all of it is entrapped by imbibing water, (2) the residual NAPL saturation is a function of the saturation-path history (not a constant), and (3) the NAPL relative permeability (k_{ro}) will approach zero as the free-NAPL saturation (S_{of}) approaches zero. To calculate fluid saturations using the revised constitutive model in numerical models, the apparent total-liquid saturation ($\bar{\bar{S}}_t$) is first determined from the air–NAPL capillary pressure and the total-liquid saturation-path history. From the apparent total-liquid saturation and the saturation-path histories, the total-liquid (S_t) and total entrapped-air (S_{ae}) saturations are determined. Next, the apparent water saturation ($\bar{\bar{S}}_w$) is determined from the NAPL–water capillary pressure and the water saturation-path history. From the apparent water saturation and the saturation-path histories, the water (S_w) and entrapped-NAPL (S_{oe}) saturations, as well as the entrapped-air saturation that resulted from advancing air–water interfaces (S_{aew}), are determined.

The next step is to determine if the apparent total-liquid saturation ($\bar{\bar{S}}_t$) needs to be adjusted because of a limiting condition. For water drainage paths, the apparent total-liquid saturation ($\bar{\bar{S}}_t$) should never be less than the sum of the apparent water saturation and the effective residual-NAPL saturation of the previous time step because residual NAPL is immobile and should not change between time steps during drainage. If it is ($\bar{\bar{S}}_t < \bar{\bar{S}}_w + \bar{S}_{or}$), then the apparent total-liquid saturation is set equal to the sum of the apparent water saturation at the current time step and the effective residual-NAPL saturation of the previous time step ($\bar{\bar{S}}_t = \bar{\bar{S}}_w + \bar{S}_{or}$). The corresponding total-liquid (S_t) and total entrapped-air (S_{ae}) saturations are then recalculated. For water imbibition paths, the apparent total-liquid saturation ($\bar{\bar{S}}_t$) should never be less than the apparent water saturation ($\bar{\bar{S}}_w$). If it is, then the apparent total-liquid saturation is set to equal the apparent water saturation ($\bar{\bar{S}}_t = \bar{\bar{S}}_w$) and the total-liquid ($S_t$) and total entrapped-air (S_{ae}) saturations are recalculated.

When the apparent total-liquid saturation equals the apparent water saturation ($\bar{\bar{S}}_t = \bar{\bar{S}}_w$), then all of the NAPL will be trapped ($S_o = S_{oe}$).

The next step is to calculate the effective residual-NAPL saturation ($\bar{S}_{or}$) at the current time step. From calculations in earlier steps, all other saturations (S_{aeo}, S_{of}, S_{or}, S_o, etc.) can be determined. These values can be used to evaluate mass balances and determine relative permeabilities. The final step is to update the historic saturations $\bar{\bar{S}}_w^{min}$ (used to determine S_{oe}), $\bar{\bar{S}}_t^{min}$, and $\bar{\bar{S}}_t^{max}$. Because an air–NAPL–water fluid system exists, the effective water saturation at the saturation-path reversal from the main $S–P$ path to a scanning water imbibition path in a two-phase air–water fluid system ($^\Delta \bar{S}_w^{aw}$) is fixed and does not need to be updated; it was established prior to NAPL imbibition.

It is expected that the presented modifications will yield more accurate predictions of NAPL behavior in the vadose zone. The revised model is applicable to NAPLs less dense than water (LNAPLs) and NAPLs more dense than water (DNAPLs). Although we have stated that the revised model pertains to the vadose zone (an air–NAPL–water fluid system), it can be used, like the existing model, to predict fluid behavior in two-phase air–water and NAPL–water systems. The model can be also used for both spreading and nonspreading NAPLs because the different behavior should be accounted for by the calibration term ($\bar{S}_{or}^{max}$) in Eq. (10).

As an initial test of our predictive equation for residual NAPL, we compare predictions using Eq. (10) to experimental data recently published by van Geel and Roy (2002), who used a spreading NAPL (heptane mixed with Sudan III dye). In the experiments, van Geel and Roy (2002) measured the residual-NAPL saturation at three different water saturations on the main drainage $S–P$ branch with varying initial NAPL saturations. One set of measurements was conducted at the residual-water saturation. We obtained the calibration parameter S_{or}^{max} by using Eq. (10) for experiments with an apparent water saturation of 0 (i.e., $S_w = S_{wr}$) and a historic maximum apparent total-liquid saturation ($\bar{\bar{S}}_t^{max}$) of 1 ($\bar{\bar{S}}_t = 1$ as an initial condition). The resulting S_{or}^{max} was 0.173. We used the average value of the five replicates measured by van Geel and Roy (2002) for each experimental condition in all of our calculations.

Table 1
Comparison of predicted and measured residual-NAPL saturation

$\bar{\bar{S}}_t^{max}$	S_{or} (predicted)	S_{or} (measured)
For water saturation = residual-water saturation		
0.69	0.144	0.148
0.51	0.123	0.128
0.27	0.089	0.105
For water saturation = 0.20		
0.68	0.135	0.136
0.52	0.117	0.120
0.29	0.085	0.090
For water saturation = 0.40		
0.84	0.082	0.147
0.53	0.055	0.091

For the experimental conditions given in van Geel and Roy (2002), the experimental historic maximum apparent total-liquid saturation ($\bar{\bar{S}}_t^{max}$), the measured residual-NAPL saturation (S_{or}), and the predicted residual-NAPL saturations (S_{or}) using Eq. (10) are given in Table 1. Comparisons are made for all experimental conditions given by van Geel and Roy (2002), except for when the apparent total-liquid saturation ($\bar{\bar{S}}_t$) is 1 (liquid-saturated conditions). The latter measurements were used to obtain the maximum residual-NAPL saturation (S_{or}^{max}). The predicted and measured residual-NAPL saturations (S_{or}) compare favorably, suggesting that Eq. (10) is capable of accurately predicting the residual-NAPL saturation for varying water and NAPL saturations using a spreading NAPL.

The largest discrepancies in Table 1 between predicted and measured residual-NAPL saturations (S_{or}) are at the highest water saturation (i.e., $S_w = 0.4$). However, these discrepancies are not significant. For example, the average measured residual-NAPL saturation (S_{or}) was 0.147 when the water saturation was 0.4 ($S_w = 0.4$) and the experimental historic maximum apparent total-liquid saturation was 0.84 ($\bar{\bar{S}}_t^{max} = 0.84$). Our predicted S_{or} of 0.082 is within the 95% confidence interval of the average measured value and relatively close to the lowest measured value, which was 0.099 (van Geel and Roy, 2002). For $S_w = 0.4$ and $\bar{\bar{S}}_t^{max} = 0.53$, the lowest measured S_{or} of the five replicates was 0.072. Our corresponding predicted S_{or} (0.055) was within the 95% confidence interval of the average measured value and was again relatively close to the lowest measured value (less than two saturation units).

These results give a preliminary indication that Eq. (10) is capable of predicting residual NAPL as a function of saturation-path history. We are encouraged that our assumption that the residual-NAPL saturation (S_{or}) is a function of the apparent water saturation ($\bar{\bar{S}}_w$) may be correct. Van Geel and Roy (2002) found that the residual-NAPL saturation (S_{or}) was not a function of the water saturation (S_w), but rather a function of the maximum NAPL saturation prior to drainage. Further experimental data are needed, especially the kind reported by van Geel and Roy (2002) to gain a better understanding of the formation of residual NAPL.

As another test of the proposed model, saturations and the NAPL relative permeabilities are calculated using the modified $k-S-P$ relations for a scenario involving NAPL imbibition into a two-phase air–water system and subsequent NAPL drainage to its residual saturation. Parameters used in the calculations reflect a sandy porous medium (Table 2). The maximum residual-NAPL saturation (S_{or}^{max}) employed in the analyses is 0.2. The maximum entrapped-air saturation that resulted from advancing air–NAPL interfaces corresponding to the main NAPL imbibition saturation path in a two-phase air–NAPL system is given by $^iS_{aeo}$. The maximum entrapped-air saturation that resulted from advancing air–water interfaces corresponding to the main water imbibition saturation path

Table 2
Parameters used to calculate saturations for the hypothetical saturation-path scenario

Parameter	Value	Parameter	Value	Parameter	Value
α^d	0.05 cm^{-1}	β_{ao}	1.8	$^iS_{aeo}$	0.20
α^i	0.10 cm^{-1}	β_{ow}	2.25	$^iS_{aew}$	0.25
n	2.0	S_{or}^{max}	0.20		
S_{wr}	0.15				

in a two-phase air–water system is given by $^iS_{aew}$. Both $^iS_{aeo}$ and $^iS_{aew}$ are used to calculate the entrapped air in the free NAPL (see Lenhard, 1992, for a general description). All values in Table 2 are arbitrary, but reflect a spreading NAPL in a sandy porous medium.

Inputs into the modeling exercise at each step are of the air–NAPL and NAPL–water capillary pressures and pertinent saturation-path parameters. In our scenario, NAPL imbibition occurs at a water saturation (S_w) of 0.356 on the main water drainage saturation path. At the inception of the three-phase air–NAPL–water fluid system, the corresponding air–NAPL and NAPL–water capillary heads are 44.4 and 35.5 cm of water, respectively. NAPL imbibition continues until the air–NAPL capillary head becomes equal to 3 cm of water. Thereafter, NAPL drainage ensues and the air–NAPL capillary head increases. To simplify the calculations and analyses, the water saturation (S_w) is assumed to be constant, i.e., the NAPL–water capillary head remains at 35.5 cm of water throughout the exercise.

Fig. 4A shows how the total-liquid (S_t) and water (S_w) saturations change as NAPL imbibes into the porous medium. The total-liquid saturation (S_t) increases as the air–NAPL capillary head decreases from 44.4 to 3 cm of water. The water saturation (S_w) remains constant. At early stages of NAPL imbibition, all of the NAPL is predicted to be in residual form (Fig. 4B). This is reasonable because the initial NAPL imbibing into a
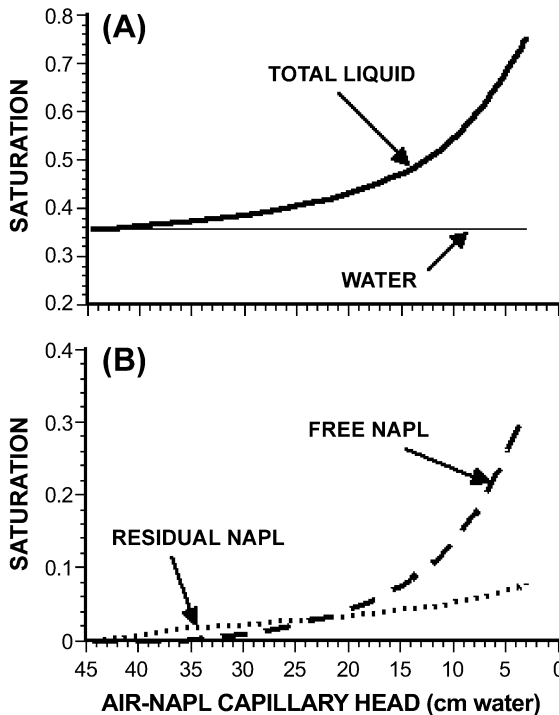

Fig. 4. Predictions of the total-liquid (thick line), water (thin line), residual-NAPL (dotted line), and free-NAPL (broken line) saturations as a function of the air–NAPL capillary head for the hypothetical scenario during NAPL imbibition.

two-phase air–water fluid system will first occupy smaller pore spaces (pore wedges) and form NAPL films before occupying larger spaces. As it occupies those smaller spaces, we assume that it is immobile, i.e., at low NAPL saturations, we assume the NAPL to be immobile (residual). Free NAPL is calculated to appear after the total-NAPL saturation (S_o) becomes approximately 0.015 (Fig. 4B), which is a relatively low value. The total-NAPL saturation at which free NAPL appears depends on the porous medium properties and the water and total-liquid saturation-path histories. As the total-NAPL saturation continues to increase, the rate of increase in free NAPL exceeds that of residual NAPL. This is also reasonable because the ratio of larger pore space, which will contain free NAPL, to pore-wedge space and NAPL film area, which will contain residual NAPL, will increase as NAPL invades larger pores. The residual-NAPL saturation (S_{or}) continues to increase as the total-NAPL saturation (S_o) increases because more pore-wedge space and NAPL film area becomes filled with NAPL as it invades those larger pore spaces that are inaccessible to the NAPL when the NAPL saturation is lower. At an air–NAPL capillary head of approximately 23 cm of water (Fig. 4B), the free- (S_{of}) and residual-NAPL (S_{or}) saturations are the same (0.03). At an air–NAPL capillary head of 3 cm of water, the free-NAPL saturation (S_{of}) is 0.319 and the residual-NAPL saturation (S_{or}) is 0.078.
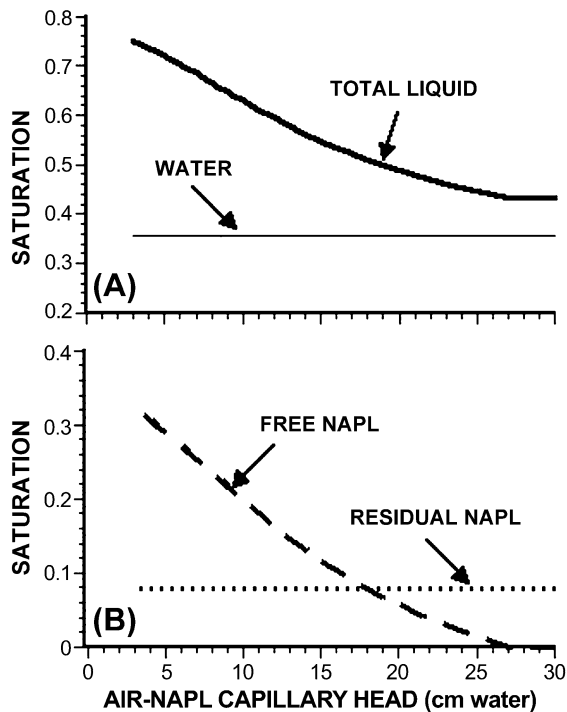

Fig. 5. Predictions of the total-liquid (thick line), water (thin line), residual-NAPL (dotted line), and free-NAPL (broken line) saturations as a function of the air–NAPL capillary head for the hypothetical scenario during NAPL drainage.

Fig. 5A shows how the total-liquid (S_t) and water (S_w) saturations change as NAPL drains to its residual value. As the air–NAPL capillary head increases, the total-liquid saturation decreases. The decrease in the free-NAPL saturation (S_{of}) in Fig. 5B is mirrored by the decrease in the total-liquid saturation (S_t) in Fig. 5A because the water (S_w) and residual-NAPL saturations (S_{or}) are time-invariant. The residual-NAPL saturation (S_{or}) in Fig. 5B is constant during NAPL drainage because the historic maximum apparent total-liquid saturation ($\bar{\bar{S}}_t^{max}$) and the apparent water saturation ($\bar{\bar{S}}_w$) do not change (see Eq. (10)). It is reasonable that the residual-NAPL saturation is constant for this saturation path because the NAPL in the NAPL-filled pore wedges is immobile. The pore-wedge space was filled during NAPL imbibition. Only the adjacent free NAPL in the pores will drain as the air–NAPL capillary head increases. We assume that residual NAPL in bypassed pores is indirectly accounted for by the calibration term (S_{or}^{max}). In any later refinements of the residual NAPL model, another term may need to be added to Eq. (10) to directly account for NAPL in pores that is bypassed during NAPL drainage and remains in the vadose zone.

As the air–NAPL capillary head continues to increase in the hypothetical scenario, the free-NAPL saturation (S_{of}) approaches zero. In Fig. 5B, this occurs at an air–NAPL capillary head of approximately 27 cm of water. If the predicted air–NAPL capillary head increases further, then the apparent total-liquid saturation ($\bar{\bar{S}}_t$) is constrained to equal the sum of the apparent water saturation at the current time step and the effective residual-NAPL saturation of the previous time step ($\bar{\bar{S}}_t = \bar{\bar{S}}_w + \bar{S}_{or}$). Under this condition, the free-NAPL saturation (S_{of}) is predicted to be zero and NAPL is not allowed to drain from the system because its relative permeability is zero.

Fig. 6 shows how the predicted NAPL relative permeabilities (k_{ro}) vary during the NAPL imbibition and drainage scenario. The arrows show the direction of NAPL movement. Because of the way in which the formation of residual NAPL is modeled,
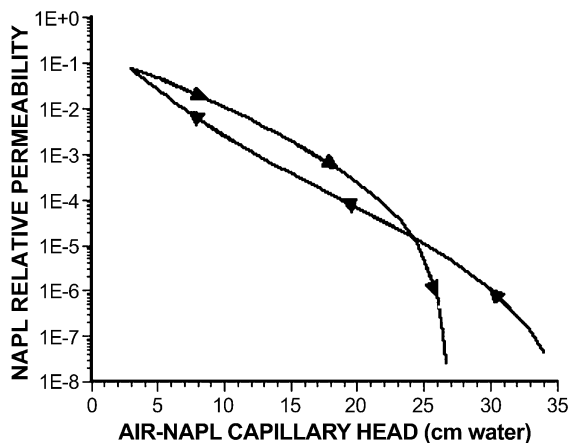

Fig. 6. Predictions of the NAPL relative permeability as a function of the air–NAPL capillary head for the hypothetical scenario involving NAPL imbibition and drainage.

there is hysteresis in the predicted NAPL relative permeabilities. However, the hysteresis shown in Fig. 6 is not entirely a result of how we model residual NAPL. Some of the hysteresis is attributed to hysteresis in the $S-P$ relations. The $k-P$ behavior shown in Fig. 6 is complex because the relations between the apparent total-liquid saturation ($\bar{\bar{S}}_t$) and the air–NAPL capillary pressure are hysteretic and relations between the free-NAPL saturation (S_{of}) and the total-liquid saturation (S_t) are hysteretic. A partial explanation of the $k-P$ hysteretic behavior is that the amount of residual NAPL relative to the total-NAPL saturation (S_o) is higher on NAPL drainage paths than on NAPL imbibition paths. This occurs because as NAPL imbibes into larger pore spaces, the NAPL has access to more pore wedges in which it becomes immobile. On drainage paths, the NAPL never drains from these pore-wedge spaces, so that the ratio of residual to free NAPL is greater on drainage paths than on imbibition paths. When the free-NAPL saturation (S_{of}) approaches zero, the NAPL relative permeability (k_{ro}) will rapidly approach zero (see Fig. 6). The rate at which it approaches zero will depend on the pore sizes (radii) containing the free NAPL. Results of the modeling exercise are consistent with our conceptual model of residual NAPL formation and the effects it has on $k-S-P$ relations.

5. Summary and conclusions

A mathematical model for predicting residual NAPL in three-phase air–NAPL–water fluid systems was developed. The model was incorporated into an existing hysteretic $k-S-P$ model for predicting subsurface fluid flow. Modifications to the existing $k-S-P$ model were minimized to allow easy coding changes. The conceptual model of residual NAPL formation used for the mathematical model is that NAPL becomes immobile when it forms thin films and when it invades small pore spaces, such as pore wedges. Therefore, the residual-NAPL saturation will increase as NAPL invades more pore volume because more pore-wedge space will become accessible and the potential NAPL-film area will become larger. During NAPL drainage, the NAPL held in the pore wedges and that in thin films (residual NAPL) will not drain. Residual NAPL in the vadose zone is modeled using concepts similar to those used to model residual water in the vadose zone. The conceptual model was developed to help explain residual NAPL observed in experiments.

To test the mathematical model and modified $k-S-P$ relations, predictions of the residual-NAPL saturation were compared to published $S-P$ measurements, and analyses of predicted NAPL saturations and relative permeabilities were conducted for a hypothetical scenario involving NAPL imbibition into a two-phase air–water system and subsequent NAPL drainage. The comparison between predicted and experimental residual-NAPL saturations showed good agreement. In all cases, the predicted values were within the 95% confidence level of the measured values. In some cases, the predicted values were very close to the measured residual-NAPL saturations. The analyses of the predicted NAPL saturations and relative permeabilities for the hypothetical saturation-path scenario suggest that the modified $k-S-P$ relations can be used to predict residual NAPL in the vadose zone. The change in NAPL saturations and relative permeabilities were consistent with our conceptual model of residual NAPL.

Additional testing of the modified k–S–P model is required before it can be routinely used to predict subsurface NAPL behavior. It needs to be tested against both static S–P and transient flow air–NAPL–water measurements involving both spreading and non-spreading NAPLs. Some of the parameters (power law exponents) used in Eq. (5) were first approximations, and further refinements may be necessary. Furthermore, an additional term may be needed to directly model residual NAPL in bypassed pores, which will cause the effective residual-NAPL saturation to increase during NAPL drainage.

Developing improved constitutive theory is a method for incorporating more physics and chemistry into flow and transport predictions, especially when using continuum-based predictive models. The complex issues associated with the formation, dissolution, and volatilization of entrapped, free, and residual NAPL in two- and three-fluid phase systems cannot be described by simplistic k–S–P relations. Only by testing models against experimental data can we learn more about governing mechanisms and processes that will help us in our efforts to more accurately predict subsurface fluid flow and chemical transport. A stepwise approach is needed that involves improving and testing constitutive theory so that more accurate predictions of field-scale NAPL behavior can be obtained.

List of Symbols

S_w	water saturation
$\bar{\bar{S}}_w$	apparent water saturation
$\bar{\bar{S}}_w^{min}$	historic minimum apparent water saturation
S_{wr}	residual-water saturation
$^{\Delta}\bar{S}_w^{aw}$	effective water saturation at the saturation-path reversal from the main saturation–pressure (S–P) path to a scanning water imbibition path in a two-phase air–water fluid system
S_o	total-NAPL saturation
S_{oe}	entrapped-NAPL saturation (water-occluded)
S_{of}	free-NAPL saturation (mobile NAPL)
$\bar{S}_{of}$	effective free-NAPL saturation
S_{or}	residual-NAPL saturation
$\bar{S}_{or}$	effective residual-NAPL saturation
S_{or}^{max}	maximum residual-NAPL saturation
$\bar{S}_{or}^{max}$	effective maximum residual-NAPL saturation
S_{ae}	total-entrapped air saturation
S_{aew}	entrapped-air saturation in water (includes trapped air in NAPL that is occluded by water)
S_{aeo}	entrapped-air saturation in free NAPL (NAPL not occluded by water)
$\bar{S}_{aeo}$	effective entrapped-air saturation in free NAPL
$\bar{S}_{aeo}^{max}$	effective maximum entrapped-air saturation by advancing air–NAPL interfaces (a function of $\bar{\bar{S}}_t^{min}$ and $^iS_{aeo}$)
$\bar{S}_{aew}^{max}$	effective maximum entrapped-air saturation by advancing air–water interfaces (a function of $^{\Delta}\bar{S}_w^{aw}$ and $^iS_{arw}$)
$^iS_{aeo}$	maximum entrapped-air saturation by advancing air–NAPL interfaces corresponding to the main S–P imbibition path in a two-phase air–NAPL fluid system

$^{i}S_{aew}$	maximum entrapped-air saturation by advancing air–water interfaces corresponding to the main $S-P$ imbibition path in a two-phase air–water fluid system
$\bar{\bar{S}}_{t}$	apparent total-liquid saturation
$\bar{\bar{S}}_{t}^{max}$	historic maximum apparent total-liquid saturation
$\bar{\bar{S}}_{t}^{min}$	historic minimum apparent total-liquid saturation
$\bar{S}_{e}$	effective porosity in which the flow of fluids under consideration can potentially occur expressed as a saturation
k_{ro}	NAPL relative permeability
α^{i}	parameter in the van Genuchten (1980) $S-P$ equation for the main imbibition path
α^{d}	parameter in the van Genuchten (1980) $S-P$ equation for the main drainage path
n	shape parameter in the van Genuchten (1980) $S-P$ equation for both drainage and imbibition paths
m	van Genuchten (1980) $S-P$ equation parameter; $m = 1 - 1/n$
β_{ao}	air–NAPL scaling factor for $S-P$ relations
β_{ow}	NAPL–water scaling factor for $S-P$ relations

Acknowledgements

References

Anderson, W.G., 1987. Wettability literature survey—Part 6: the effect of wettability on waterflooding. J. Pet. Technol. 39, 1605–1622.

Burdine, N.T., 1953. Relative permeability calculations from pore-size distribution data. Pet. Trans., Am. Inst. Mining Metall. Eng. 198, 71–77.

Busby, R.D., Lenhard, R.J., Rolston, D.E., 1995. An investigation of saturation-capillary pressure relations in two- and three-fluid systems for several NAPLs in different porous media. Ground Water 33, 570–578.

Cary, J.W., McBride, J.F., Simmons, C.S., 1989. Trichloroethylene residuals in the capillary fringe as affected by air-entry pressure. J. Environ. Qual. 18, 72–77.

Cohen, R.M., Mercer, J.W., 1993. DNAPL Site Evaluation. CRC Press, Boca Raton, FL.

Hofstee, C., Dane, J.H., Hill, W.E., 1997. Three-fluid retention in porous media involving water PCE, and air. J. Contam. Hydrol. 25, 235–247.

Hofstee, C., Walker, R.C., Dane, J.H., 1998. Infiltration and redistribution of perchloroethylene in partially saturated, stratified porous media. J. Contam. Hydrol. 34, 293–313.

Jarsjo, J., Destouni, G., Yaron, B., 1994. Retention and volatilization of kerosene: laboratory experiments on glacial and post-glacial soils. J. Contam. Hydrol. 112, 586–604.

Kovscek, A.R., Wong, H., Radke, C.J., 1993. A pore-level scenario for the development of mixed wettability in oil reservoirs. AIChE J. 39, 1072–1085.

Lenhard, R.J., 1992. Measurement and modeling of three-phase saturation–pressure hysteresis. J. Contam. Hydrol. 9, 243–269.

Lenhard, R.J., Parker, J.C., 1987. A model for hysteretic constitutive relations governing multiphase flow: 2. Permeability–saturation relations. Water Resour. Res. 23, 2197–2206.

Lenhard, R.J., Parker, J.C., 1988. Experimental validation of the theory of extending two-phase saturation–pressure relations to three-phase systems for monotonic drainage paths. Water Resour. Res. 24, 373–380.

Morrow, N.R., 1990. Wettability and its effect on oil recovery. J. Pet. Technol. 42, 1476–1484.

Mualem, Y., 1976. A new model for predicting the hydraulic conductivity of unsaturated porous media. Water Resour. Res. 12, 513–522.

Oostrom, M., Lenhard, R.J., 2003. Carbon tetrachloride flow behavior in unsaturated Hanford caliche material: an investigation of residual NAPL. Vadose Zone J. 2, 25–33.

Oostrom, M., Hofstee, C., Lenhard, R.J., Wietsma, T.W., 2003. Flow behavior and residual saturation formation of liquid carbon tetrachloride in unsaturated heterogeneous porous media. J. Contam. Hydrol. 64, 93–112.

Parker, J.C., Lenhard, R.J., 1987. A model for hysteretic constitutive relations governing multiphase flow: 1. Saturation–pressure relations. Water Resour. Res. 23, 2187–2196.

Poulsen, M.M., Kueper, B.H., 1992. A field experiment to study the behavior of tetrachloroethylene in unsaturated porous media. Environ. Sci. Technol. 26, 889–895.

Rapoport, L.A., Leas, W.J., 1951. Relative permeability to liquid in liquid–gas systems. Trans. AIME 192, 83–98.

Rose, W., 1949. Theoretical generalizations leading to the evaluation of relative permeability. Trans. AIME 186, 111–126.

Rose, W., Bruce, W.A., 1949. Evaluation of capillary character in petroleum reservoir rock. Trans. AIME 186, 127–142.

Salathiel, R.A., 1973. Oil recovery by surface film drainage in mixed-wettability rocks. J. Pet. Technol. 25, 1216–1224.

van Geel, P.J., Roy, S.D., 2002. A proposed model to include a residual NAPL saturation in a hysteretic capillary pressure–saturation relationship. J. Contam. Hydrol. 58, 79–110.

van Genuchten, M.Th., 1980. A closed-form equation for predicting the hydraulic conductivity of unsaturated soils. Soil Sci. Soc. Am. J. 44, 892–898.

Willhite, G.P., 1986. Waterflooding Society of Petroleum Engineers, Richardson, TX.

Wipfler, E.L., van der Zee, S.E.A.T.M., 2001. A set of constitutive relationships accounting for residual NAPL in the unsaturated zone. J. Contam. Hydrol. 50, 53–77.

Wyllie, M.R.J., Sprangler, M.B., 1952. Applications of electrical resistivity measurement to problems of fluid flow in porous media. Bull. AAPG 36, 359.